AJNR

Alteration of cerebral blood flow in patients with bacterial and viral meningoencephalitis.

S Merkelbach, M Müller, G Huber and K Schimrigk

AJNR Am J Neuroradiol 1998, 19 (3) 433-438
http://www.ajnr.org/content/19/3/433

AJNR Am J Neuroradiol 19:433–438, March 1998

Alteration of Cerebral Blood Flow in Patients with Bacterial and Viral Meningoencephalitis

Stefan Merkelbach, Martin Müller, Gisela Huber, and Klaus Schimrigk

PURPOSE: **Our purpose was to investigate cerebral blood flow disturbances in patients with bacterial and viral meningoencephalitis.**

METHODS: **Forty-two patients with acute bacterial and viral meningoencephalitis and 14 control subjects were studied using ^{99m}Tc-hexamethylpropyleneamine oxime (HMPAO) single-photon emission computed tomography (SPECT). SPECT images were evaluated semiquantitatively. The results were compared with clinical severity of the meningoencephalitis assessed at the time of the SPECT study with the Hunt and Hess scale, with separately recorded focal clinical signs, and with the Glasgow outcome scale (GOS) after 3 weeks.**

RESULTS: **Count density values were significantly reduced in patients with bacterial meningoencephalitis as compared with the control subjects. Inhomogeneous tracer accumulation assessed by asymmetry indexes was significantly greater in patients than in the control group. With increasing Hunt and Hess scores, the count density values decreased and the asymmetry indexes increased. Patients with a poor outcome (GOS 1 to 3) had significantly higher asymmetry indexes and lower CDV values than did patients with a good outcome.**

CONCLUSION: **Global and focal alterations of cerebral perfusion are frequent in bacterial and viral meningoencephalitis and correlate with acute clinical state.**

The clinical course of bacterial and viral meningoencephalitis can be accompanied by such complications as brain edema; impairment of CSF resorption leading to hydrocephalus; brain abscesses; cerebrovascular alterations, such as stenoses and arterial occlusions; brain infarctions; and dural sinus thrombosis (1, 2). Vascular complications in bacterial meningoencephalitis have been offered as one possible explanation for the high rate of neurologic sequelae among survivors. Several angiographic studies have revealed stenoses or occlusions of the intracranial vessels in these patients (3–5).

Noninvasive imaging techniques, such as transcranial Doppler sonography, have shown highly elevated mean blood velocities in the basal cerebral arteries (6–8). These findings may be interpreted as vasospasm, and inflammatory thickening of the walls of the basal cerebral vessels by vasculitic changes must be considered a further possible cause of reduction in vessel diameter (9, 10). Transcranial Doppler sonographic studies may, however, only depict alterations in the proximal branches of the cerebral arteries (11). One advantage of noninvasive nuclear imaging methods is that they allow the visualization of disturbances of cerebral blood flow (CBF) caused by changes in the microcirculation (12–14). CBF in bacterial and viral meningoencephalitis has been reported to be reduced globally and regionally as a consequence either of an inflammatory process or its complications (15–17).

We report our experience with the use of quantitative region-of-interest (ROI) technology in the evaluation of CBF in patients with bacterial and viral meningoencephalitis and compare our results with the clinical findings in these patients.

Methods

Patients

Forty-two patients (20 men and 22 women; mean age ± SD, 50 ± 16 years) with the clinical diagnosis of bacterial (n = 15) or viral (n = 27) meningoencephalitis were included in the study. Fourteen healthy volunteers (seven men and seven women; mean age ± SD, 53 ± 20 years) were studied as control subjects. The diagnosis of meningoencephalitis was based on clinical signs and symptoms, including severe headache, stiffness of the neck, disturbed levels of consciousness, fever of more than 38.5°C, and appropriate CSF findings. Smears stained with May-Grünwald-Giemsa were used for differential leucocyte count.

Bacterial meningitis was diagnosed when the CSF exhibited a polymorphonuclear pleocytosis of more than 1000 cells/μL, or a bacterial pathogen was identified by CSF cultures (1, 7). The causative bacterial pathogens were *Streptococcus pneumoniae* in seven patients, *Listeria monocytogenes* in one patient,

Received April 1, 1997; accepted after revision September 19.

From the Department of Neurology (S.M., M.M., K.S.) and the Institute of Neuroradiology (G.H.), University Hospital of the Saarland, Homburg/Saar, Germany.

Address reprint requests to Stefan Merkelbach, MD, Department of Neurology, University Hospital of the Saarland, Oscar-Orth-Str. 3, D-66421 Homburg/Saar, Germany.

Neisseria meningitidis in one patient, *Escherichia coli* in one patient, *Borrelia burgdorferi* in one patient, *Mycobacterium tuberculosis* in one patient, and unknown in three patients.

Viral meningoencephalitis was assumed in the presence of a lymphocytic pleocytosis of less than 1000 cells/μL (8). On the basis of serologic antibody titer investigation or characteristic clinical findings, it was determined that two patients had varicella-zoster viral infection and two had mumps infection. In one patient, tick-borne encephalitis virus was the suspected pathogen; and, in the remaining 22 patients, the viral pathogen could not be identified. Herpes simplex viral encephalitis was not confirmed in any patient.

The clinical severity of the disorder at the time of single-photon emission computed tomography (SPECT) was classified with the use of the Hunt and Hess scale, as follows: 1 = asymptomatic, or minimal headache and slight nuchal rigidity; 2 = moderate or severe headache, nuchal rigidity, no neurologic deficit except cranial nerve palsy; 3 = drowsiness, confusion, or mild cerebral deficit; 4 = stupor, moderate or severe hemiparesis, possible early decerebrate rigidity, and vegetative disturbances; and 5 = deep coma, decerebrate rigidity, moribund (18). The control subjects were considered to have a Hunt and Hess grade of 0. The Hunt and Hess scale was chosen because the primary involvement of meninges and the development of macrovascular changes in patients with bacterial meningoencephalitic are similar to those seen in patients with subarachnoid hemorrhage. Special attention was paid to signs such as hemiparesis, hemihypesthesia, hemineglect (ie, the phenomenon of hemiextinction on bilateral simultaneous stimulation), aphasia, and focal seizures. Outcome was determined using the Glasgow Outcome Scale (GOS): 1 = death, 2 = persistent vegetative state, 3 = severe neurologic deficit, 4 = slight neurologic deficit, and 5 = complete recovery (19). The control subjects were considered to have a GOS of 5.

Patients with bacterial meningoencephalitis were treated with standardized antibiotic combinations consisting of penicillin G, cefotaxime sodium, and gentamicin, which were adapted according to microbiological susceptibility. Patients with viral meningoencephalitis were treated with acyclovir if herpes simplex virus was the suspected pathogen. If indicated, intensive-care therapy, including treatment with hyperosmolar substances and artificial ventilation, was initiated in both subgroups.

Procedures

Regional CBF was evaluated by ^{99m}Tc-hexamethylpropyleneamine oxime (HMPAO) SPECT. SPECT studies were performed within 1 to 14 days (mean ± SD, 4 ± 3 days) after admission. This period was defined as the acute phase of the infectious disease, because clinical cerebral complications as well as hemodynamic disturbances on transcranial Doppler sonograms are common within this period (6–8). Informed consent was obtained from the patients or their guardians. The study was approved by the local institutional ethics committee.

For each SPECT study, data acquisition over 20 minutes was started 5 minutes after intravenous injection of about 370 mBq of ^{99m}Tc-HMPAO using a single-headed rotating camera. Tracer activity was measured using a becquerel meter (PTW-Curiementor, Freiburg, Germany). Per patient, 3.342 ± 0.679×10^6 counts (range, 2.059 to 5.070×10^6 counts) were collected. We used a matrix size of 64 × 64 pixels and 60 projections over 360° (6° angular steps). After the images were reconstructed by filtered back-projection, transverse, sagittal, and coronal sections were processed. The resulting thickness of the color-coded sections was 12 mm. Spatial resolution, including collimator, was 9 mm.

After visual qualitative evaluation of gross asymmetries of tracer accumulation, we performed a quantitative analysis of tracer distribution with the use of a mask, on which 24 defined ROIs with identical areas were established, 11 for each cerebral hemisphere and one for each cerebellar hemisphere. From reconstructed transverse sections, one section each was selected for CBF measurement at the infratentorial, thalamic, paraventricular, and supraventricular levels to quantify HMPAO uptake in the frontal, temporal, parietal, and occipital lobes, the cerebellar gray matter, and the temporal white matter (Fig 1). Each ROI on the mask was applied automatically by a computerized system and later adjusted manually. The SPECT analysis was performed by an examiner who was blinded to the clinical data.

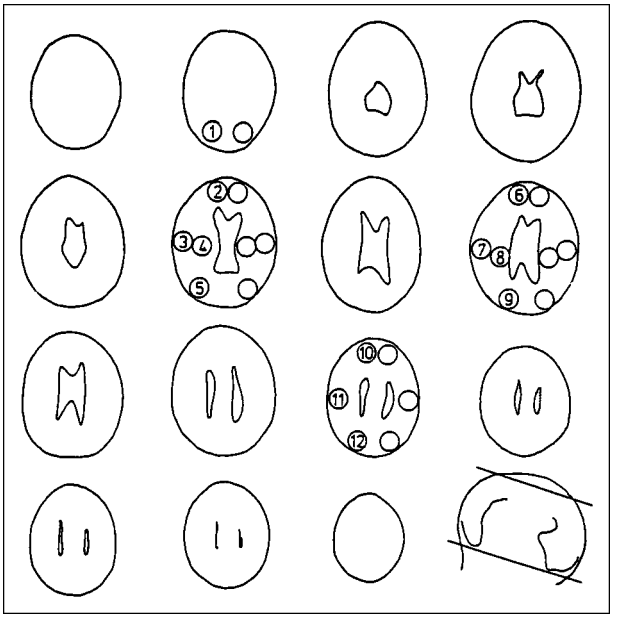

FIG 1. Topography of standardized ROI projection on SPECT sections.

The count density value (CDV) was measured for each ROI as counts per pixel. Ratios of all cerebral ROIs with cerebellar reference ROIs were calculated by dividing supratentorial CDV values through the cerebellar CDV value, because cerebellar perfusion seems to show small variations under various pathologic conditions (20). Because cerebellar perfusion may be influenced by cerebral lesions of the contralateral hemisphere owing to crossed cerebellar diaschisis, we used ipsilateral cerebellar ROIs as references (21). A mean CDV was calculated for each patient based on all ROIs and for each ROI in all patients.

According to Tranquart and coworkers (22) indexes of asymmetric perfusion were calculated as ratios of tracer accumulation between paired right (r) and left (l) symmetric ROIs (asymmetry index, AI) as follows:

$$AI = [(CDV_{ROIr} - CDV_{ROIl})/(CDV_{ROIr} + CDV_{ROIl})] \times 200$$

A regional disturbance of CBF was identified when the AI of one pair of ROIs was higher than 10%. The AIs were analyzed in two ways. First, in each patient, the individual mean AI was calculated and, in addition, the number of AIs with a deviation of more than 10% was counted (the number of AIs). Second, in all patients, regional asymmetries were studied by calculating the mean AI for each ROI (regional mean AI).

Statistical Analysis

All values are reported as mean ± SD. Using the Kolmogorov-Smirnov test, we distributed the CDV values and the AI values in patients and control subjects showed normal distribution. CDV, cerebellar CDV ratios, individual mean AI, and regional mean AI of patients with bacterial and viral meningoencephalitis were compared with those of the control group by using Student's t-test. Because of the multiple testing proce-

TABLE 1: Count Density Values for Each Region of Interest in Patients with Bacterial and Viral Meningoencephalitis and in Healthy Control Subjects

ROI	CDV ± SD (*P* Value)		
	Control Subjects	Patients with Meningoencephalitis	
		Bacterial	Viral
1	6949 ± 1098	5722 ± 905 (.0005)	6582 ± 1696 (.238)
2	6043 ± 890	4982 ± 743 (.0005)	5707 ± 1434 (.193)
3	5854 ± 911	4790 ± 755 (.0005)	5675 ± 1461 (.516)
4	5307 ± 927	4536 ± 749 (.0005)	5270 ± 1537 (.784)
5	5920 ± 952	5088 ± 852 (.001)	5731 ± 1552 (.495)
6	5961 ± 924	4865 ± 704 (.0005)	5570 ± 1457 (.242)
7	5750 ± 831	4847 ± 759 (.0005)	5645 ± 1636 (.697)
8	4782 ± 909	4129 ± 760 (.003)	4731 ± 1550 (.784)
9	5785 ± 1144	4960 ± 786 (.001)	5709 ± 1498 (.799)
10	5562 ± 866	4580 ± 849 (.0005)	5251 ± 1393 (.214)
11	5625 ± 895	4876 ± 800 (.001)	5512 ± 1356 (.650)
12	5952 ± 940	5094 ± 826 (.0005)	5813 ± 1593 (.619)
Mean CDV	5782 ± 895	4860 ± 671 (.003)	5600 ± 1495 (.062)

Note.—Values are given as mean ± SD; statistical significance was assessed using Student's t-test; ROI indicates region of interest; CDV, count density value (measured as counts per ROI).

TABLE 2: Mean Asymmetry Index for Each Region of Interest for Patients with Bacterial and Viral Meningoencephalitis and for Healthy Control Subjects

ROI	Regional Mean Asymmetry Index ± SD (*P* Value)		
	Control Subjects	Patients with Meningoencephalitis	
		Bacterial	Viral
1	3.63 ± 3.01	3.84 ± 1.88 (.844)	5.25 ± 4.06 (.162)
2	4.22 ± 4.00	5.56 ± 3.38 (.239)	6.11 ± 3.34 (.090)
3	4.27 ± 2.71	9.39 ± 5.59 (.002)	8.17 ± 6.64 (.011)
4	4.89 ± 2.37	8.74 ± 5.78 (.016)	7.38 ± 5.66 (.455)
5	4.11 ± 3.22	9.02 ± 5.48 (.004)	5.25 ± 4.16 (.247)
6	3.87 ± 3.17	5.48 ± 4.92 (.246)	5.77 ± 4.24 (.092)
7	5.19 ± 3.07	6.31 ± 3.96 (.245)	9.00 ± 6.84 (.016)
8	6.49 ± 4.96	10.2 ± 7.01 (.095)	8.83 ± 6.10 (.202)
9	4.39 ± 4.04	6.83 ± 8.15 (.233)	6.16 ± 5.79 (.247)
10	3.71 ± 2.30	7.06 ± 5.47 (.021)	5.86 ± 4.26 (.043)
11	3.80 ± 2.26	5.87 ± 3.59 (.091)	6.11 ± 4.71 (.047)
12	4.44 ± 2.61	5.53 ± 5.33 (.246)	4.40 ± 4.96 (.970)
IMAI	4.41 ± 3.14	6.99 ± 2.33 (.001)	6.52 ± 2.30 (.001)

Note.—All values are reported as mean ± SD; *P* values are from Student's t-test; the regional mean asymmetry index is for each paired ROI for all patients. ROI indicates region of interest; IMAI, individual mean asymmetry index.

dures, the Bonferoni-correction was applied. Spearman correlation coefficient was used to analyze the relationship between global and focal disturbances of CBF (evaluated as CBF, individual mean AI, and number of AIs) and Hunt and Hess grading at the time of the investigation. The relationship between mean CDV, individual mean AI, and number of AIs and clinical outcome was analyzed using the Mann-Whitney U-test, in which outcome was classified as poor (GOS score of 1 to 3) or good (GOS score of 4 to 5).

The number of AIs and the individual mean AI were compared with respect to patients with focal cerebral signs (symptomatic) and patients without such signs (asymptomatic) using the χ^2-test.

Results

Visual Impression

The number and extent of cortical deficits were greater in patients with meningoencephalitis than in control subjects. Cortical and subcortical perfusion disturbances with inhomogeneous tracer uptake were more common in patients with bacterial meningoencephalitis than in those with viral meningoencephalitis or in control subjects. Because visual inspection is subjective, we restricted further statistical analysis to the objective quantitative data.

Quantitative Analysis

The volunteers showed supratentorial tracer accumulation with pronounced cortical activity and reduced activity in the subcortical white matter (Table 1). Highest values were noticed in the cerebellum. There were no significant differences in tracer uptake between corresponding ROIs in the left and right hemispheres. Similarly, there were no side-to-side differences between the ratio of each ROI and the ipsilateral cerebellar reference. Values for corresponding ROIs of both hemispheres were summed, with resulting mean values of 0.93 ± 1.09 for the number of AIs and 4.41 ± 3.14 for the individual mean AIs (Table 2).

As in control subjects, HMPAO accumulation in patients with bacterial and viral meningoencephalitis had the highest CDV values in the cerebellar ROIs and the lowest values in the temporomedial ROIs.

CDV Analysis

The mean CDV was significantly reduced in the bacterial subgroup ($P \leq .003$) as compared with that in control subjects, but it was not significantly decreased in the viral subgroup (Table 1). Similar results were obtained in comparisons of regional differences (Table 1). In the bacterial subgroup, significantly reduced CDV values were observed in all ROIs, even after Bonferoni correction, with slight frontotemporal accentuation. In the viral subgroup, no significant differences were observed relative to the control group for any ROI. CDV ratios based on the cerebellar reference ROIs showed no significant difference between control subjects and patients.

AI Analysis

Twenty of 27 patients with viral meningoencephalitis and 12 of 15 patients with bacterial meningoencephalitis had AIs with a deviation of more than 10% in more than one paired ROI. This was also seen in four of 14 control subjects. The mean number of AIs for all patients with bacterial meningoencephalitis was 3.05 ± 1.98 (for control subjects, the mean was 0.93 ± 1.09; $P < .001$). For patients with viral meningoencephalitis, the mean number of AIs was 2.59 ± 2.03 ($P < .005$ versus control subjects). The highest frequency of asymmetric ROIs was observed in the temporal lobes, the lowest in the parietal lobes.

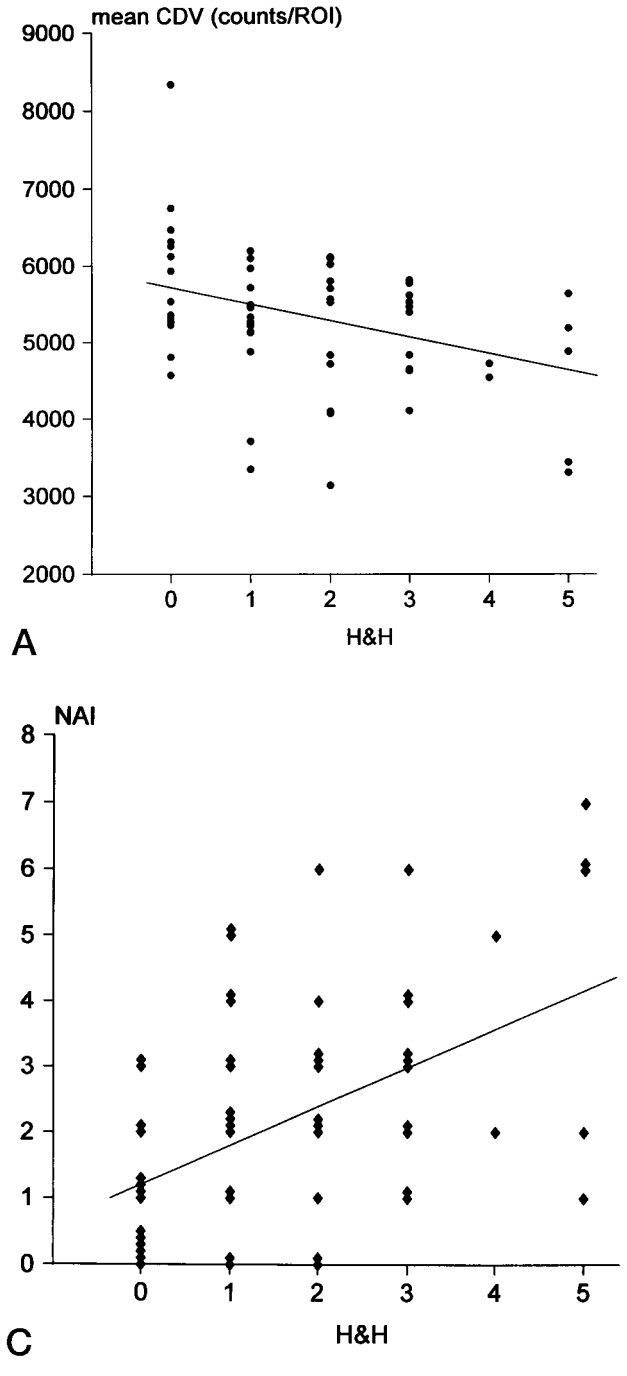

FIG 2. Correlation of quantitative SPECT parameters with the actual clinical state of the patients as measured on the Hunt and Hess (*H&H*) scale.
A, Correlation with the mean count density values (*CDV*).
B, Correlation with the individual mean asymmetry index (*IMAI*).
C, Correlation with the number of asymmetric indexes (*NAI*).

The individual mean AI was significantly higher in the bacterial and viral subgroups than in the control group ($P \leq .001$ for both bacterial and viral subgroups) (Table 2). The highest value for regional asymmetries by means of regional mean AI was found in the frontotemporal areas (ROIs 3, 4, 7, 10, 11) (Fig 1 and Table 2).

Comparison with Clinical Parameters

The mean CDV was lower in patients with higher Hunt and Hess scores than in those with lower scores ($r = -.2921$; $P < .025$; Spearman coefficient) (Fig 2A). Additionally, the cerebellar CDV decreased with increasing Hunt and Hess scores ($r = -.3154$; $P < .01$). In the patients with higher Hunt and Hess scores, individual mean AIs were higher than in patients with lower Hunt and Hess scores ($r = .4387$; $P < .0005$) (Fig 2B). Additionally, the number of AIs was significantly higher in patients with higher Hunt and Hess scores than in patients with lower grades ($r = .4368$; $P < .0005$) (Fig 2C).

Patients with focal clinical signs (n = 11) had a significantly higher number of AIs (4.0 ± 2.4) than did patients without focal signs (n = 31; 2.3 ± 1.6; $P < .025$). The individual mean AI in patients with clinical focal signs (7.7 ± 3.2) was not significantly different from that in patients without focal signs (6.2 ± 1.8).

TABLE 3: Correlation Between SPECT Parameters and Clinical Outcome

	Good Outcome (GOS 4–5; n = 48)	Poor Outcome (GOS 1–3; n = 8)	*P* Value
NAI	1.96 ± 1.50	4.13 ± 2.70	.030
IMAI	5.90 ± 1.95	8.36 ± 3.62	.043
Mean CDV	5356 ± 828	4523 ± 815	.034

Note.—NAI indicates the number of asymmetric pairs of ROIs per patient; IMAI, individual mean asymmetry index; CDV, count density value. The Mann-Whitney U-test was used for comparison.

Comparison with Time and Outcome

There was no significant correlation between CDVs, individual mean AI, or number of AIs and the time between admission and SPECT examination. Patients with a poor outcome (GOS 1 to 3) had significant higher individual mean AI values and number of AIs and significant lower mean CDVs than did patients with a good outcome (GOS 4 to 5) (Table 3).

Discussion

Technetium-99m HMPAO is a lipophilic tracer that crosses the blood-brain barrier and remains fixed in cerebral tissue (14). Brain uptake of ^{99m}Tc-HMPAO shows a rapid kinetic and prolonged retention followed by nearly unchanged distribution of radioactivity for several hours (13, 23, 24). Therefore, ^{99m}Tc-HMPAO SPECT provides tomographic images of cerebral perfusion. Extraction across the blood-brain barrier is about 75% (14). Additionally, some amount of back-diffusion of HMPAO from brain to blood or flow-dependent irregularities may affect evaluation of CBF (20, 24). Evaluation and quantification of CBF with ^{99m}Tc-HMPAO SPECT require procedures with correcting algorithms, linearization, and comparison with arterial input curves (20, 24–26). The cerebellum is often used as a reference because of its uniform flow (12). However, a contralateral reduction of cerebellar blood flow (so-called crossed cerebellar diaschisis) is seen in patients with hemispheric cortical or subcortical lesions (21). In case of bihemispheric cerebral alterations of CBF (which can be assumed in a global inflammatory process such as meningoencephalitis) both cerebellar hemispheres may show a decreased CBF (7–9, 15). This observation is supported by our findings that the count rates in the cerebellar ROIs decreased with increasing Hunt and Hess scores similar to the mean CDV. Additionally, the vertebrobasilar arterial system may also be affected by the inflammatory process (9, 27, 28). Thus, quantitative measurements using reference regions (eg, cerebellar or the whole brain tracer uptake) should be interpreted carefully when quantifying CBF with SPECT in patients with meningoencephalitis.

Our results demonstrate that focal and global CBF alterations are common in meningoencephalitis. This is consistent with previous studies using HMPAO SPECT or stable enhanced xenon CT for CBF evaluation (15–17, 29). A global reduction of CBF in children with bacterial meningoencephalitis was reported by investigators using stable enhanced xenon CT (16, 29). Our results, which showed a correlation between CBF and clinical severity as assessed by Hunt and Hess scores, may support the assumption that decreased global count rates reflect globally reduced CBF.

Additionally, there are regional alterations, which can be described as focal hyperperfusion or hypoperfusion. Launes and coworkers (17) as well as Duncan et al (30) reported focal tracer hyperaccumulation in frontal and temporal brain regions in patients with herpes simplex viral encephalitis. The presence of hyperperfusion is supported by the angiographic findings of persistent filling of terminal arteries, local blushes, staining of blood vessels, and hypervascularity (31). In experimental conditions, increased CBF due to hyperemia in the initial phase of bacterial meningoencephalitis has been noticed and may be explained by an increased metabolic turnover as a result of the inflammatory processes (9, 32, 33). In case of an impaired blood-brain barrier, the part of HMPAO that crosses the barrier may be artificially enlarged, simulating a region of focal tracer hyperaccumulation (15, 34).

Focal hypoaccumulation of radiotracer occurs more often in patients with bacterial meningitis and has recently been reported to be associated with clinical symptoms (15). Focal hypoaccumulation may be due to vascular changes in the large basal cerebral arteries as well as in the cerebral microvessels (3, 5, 9, 10, 32). Similar cerebral microvascular changes have been described in patients with varicella zoster meningoencephalitis (35). Using transcranial Doppler sonography, some researchers have noted the frequent occurrence of increased blood velocity in the cerebral arteries during the first week of bacterial meningoencephalitis and, to a lesser degree, in viral meningoencephalitis (6–8, 28).

Apart from cerebral ischemia due to arterial narrowing, cortical or subcortical hypoaccumulation of radiotracer may be caused by a decreased metabolic demand in the condition of neuronal loss, as reported in patients with persistent brain damage due to ischemia (36). As an alternative interpretation, hypoaccumulation may also depend on functional neuronal depression due to loss of excitatory impulses, analogous to the phenomenon of diaschisis (21, 37).

In our study, patients with severe meningoencephalitis as assessed by Hunt and Hess scores had lower CDVs, a higher number of AIs, and a higher individual mean AI than did patients with a less severe condition, indicating that decreased and inhomogeneous CBF might be responsible, at least in part, for the actual clinical state and the outcome of the patients. Our results lead to the supposition that patients with more regional asymmetries of CBF (as assessed by mean number of AIs) or higher values of asymmetry (as assessed by individual mean AI) may incur cerebral ischemia more often than would pa-

tients with a low degree of asymmetry. Although we found a significant correlation between outcome and global and regional CBF alterations, there was also a wide overlap between the two outcome groups, indicating that the present SPECT techniques may not allow outcome prediction for an individual patient.

The widely distributed alterations in tracer uptake as assessed by CDV, number of AIs, individual mean AI, and regional mean AI may be interpreted as impairment of CBF, which is pronounced in bacterial meningitis. Also, the induction of various mediators, such as cytokines, arachidonic acid metabolites, reactive oxygen species, platelet activating factor, and nitric oxide, may be more pronounced in bacterial meningitis (9, 10, 38, 39). Additionally, increased intracranial pressure in the initial phase of meningoencephalitis may lead to global impairment of cerebral perfusion.

Conclusion

Radiotracer accumulation was significantly reduced in patients with bacterial meningoencephalitis relative to that in control subjects. Inhomogeneous tracer accumulation assessed by asymmetry indexes was significantly more frequent in patients with bacterial and viral meningoencephalitis than in the volunteers. Regional and global SPECT alterations were more marked with increasing severity of meningoencephalitis.

References

1. Pfister HW, Feiden W, Einhäupl KM. **Spectrum of complications during bacterial meningitis in adults.** *Arch Neurol* 1992;50:575–581
2. Swatz MN. **Bacterial meningitis: more involved than just the meninges.** *N Engl J Med* 1984;311:912–914
3. Igharashi M, Gilmartin RC, Gerald B, Wilburn F, Jabbour JT. **Cerebral arteritis and bacterial meningitis.** *Arch Neurol* 1984;41: 531–535
4. Snyder RD, Stovring J, Cushing AH, Davis LE, Hardy TL. **Cerebral infarction in childhood bacterial meningitis.** *J Neurol Neurosurg Psychiatry* 1981;44:581–585
5. Leeds NE, Goldberg HI. **Angiographic manifestations in cerebral inflammatory disease.** *Radiology* 1971;98:595–604
6. Haring H-H, Rötzer H-K, Reindl H, et al. **Time course of cerebral blood flow velocity in central nervous system infection.** *Arch Neurol* 1993;50:98–101
7. Müller M, Merkelbach S, Huss GP, Schimrigk K. **Clinical relevance and frequency of transient stenosis of the middle and anterior cerebral artery in bacterial meningitis.** *Stroke* 1995;26:1399–1403
8. Müller M, Merkelbach S, Hasert K, Schimrigk K. **Transcranial Doppler ultrasound measurements in patients with viral infections of the central nervous system.** *Nervenarzt* 1995;66:754–759
9. Pfister H-W, Koedel U, Haberl RL, et al. **Microvascular changes during the early phase of experimental bacterial meningitis.** *J Cereb Blood Flow Metab* 1990;10:914–922
10. Quagliarello VJ, Long WJ, Scheld WM. **Morphological alterations of the blood brain barrier with experimental meningitis in the rat.** *J Clin Invest* 1986;77:1084–1095
11. Sekhar LN, Wechsler LR, Yonas H, Luyckx K, Obrist W. **Value of transcranial Doppler examination in the diagnosis of cerebral vasospasm after subarachnoid hemorrhage.** *Neurosurgery* 1988;22: 813–821
12. Andersen AR, Fridberg H, Schmidt JF, Hasselbalch SG. **Quantitative measurements of cerebral blood flow using SPECT and 99mTc-d,l-HM-PAO compared to xenon-133.** *J Cereb Blood Flow Metab* 1988;8:S69–S81
13. Sharp PF, Smith FW, Gemmell HG, et al. **Technetium-99m HM-PAO stereoisomers as potential agents for imaging regional cerebral blood flow: human volunteer studies.** *J Nucl Med* 1986;27: 171–177
14. Neirinckx RD, Canning LR, Piper IM, et al. **99m Tc d,l-HM-PAO: a new radiopharmaceutical for SPECT imaging of regional cerebral blood perfusion.** *J Nucl Med* 1987;28:191–202
15. Förderreuther S, Tatsch K, Einhäupl KM, Pfister HW. **Abnormalities of cerebral blood flow in the acute phase of bacterial meningitis in adults.** *J Neurol* 1992;239:431–436
16. Paulson OB, Brodersen P, Hansen EL, Kristensen HS. **Regional cerebral blood flow, cerebral metabolic rate of oxygen, and cerebrospinal fluid acid-base variables in patients with acute meningitis and with acute encephalitis.** *Acta Med Scand* 1974;196:191–198
17. Launes J, Lindroth L, Liewendahl K, Nikkinen P, Brownell AL, Iivanainen M. **Diagnosis of acute herpes simplex encephalitis by brain perfusion single photon emission computed tomography.** *Lancet* 1988;1:1188–1191
18. Hunt WE, Hess RM. **Surgical risk as related to time of intervention in the repair of intracranial aneurysms.** *J Neurosurg* 1968;28: 14–20
19. Jennett B, Bond M. **Assessment of outcome after severe brain damage.** *Lancet* 1975;1:480–484
20. Yonekura Y, Nishizawa S, Mukai T, et al. **SPECT with 99m Tc-d,l-hexamethyl-propylene amine oxime (HM-PAO) compared with regional cerebral blood flow measured by PET: effects of linearization.** *J Cereb Blood Flow Metab* 1988;8:S82–S89
21. Baron JC, Bousser MG, Comar D, Castaigne P. **"Crossed cerebellar diaschisis" in human supratentorial brain infarction.** *Am Neurol Assoc* 1980;105:459–461
22. Tranquart F, Ades PE, Groussin P, Rieant JF, Jan M, Balieu JL. **Postoperative assessment of cerebral blood flow in subarachnoid hemorrhage by means of 99m Tc-HMPAO tomography.** *Eur J Nucl Med* 1993;20:53–58
23. Costa DC, Ell PJ, Cullum I, Jarrit PH. **The in vivo distribution of 99m TC-HM-PAO in normal man.** *Nucl Med Commun* 1986;7: 647–658
24. Lassen NA, Andersen AR, Fridberg L, Poulson OB. **The retention of [99m-Tc] d,l-HMPAO in the human brain after intracarotid bolus injection: a kinetic analysis.** *J Cereb Blood Flow Metab* 1988; 8(Suppl 1):S13–S22
25. Andersen AR, Fridberg H Lassen NA, Kristensen K, Neirinckx RD. **Assessment of the arterial input curve for [99m-Tc]-d,l-HM-PAO by rapid octanol extraction.** *J Cereb Blood Flow Metab* 1988; 8(Suppl 1):S23–S30
26. Pupi A, De Cristofaro MTR, Bacciottini L, et al. **An analysis of the arterial input curve for technetium-99m-HMPAO: quantification of rCBF using single-photon emission computed tomography.** *J Nucl Med* 1991;32:1501–1506
27. Davis DO, Dilenge D, Schlaepfer W. **Arterial dilatation in purulent meningitis.** *J Neurosurg* 1970;12:112–115
28. Müller M, Merkelbach S, Schimrigk K. **Cerebral hemodynamics in the posterior circulation of patients with bacterial meningitis.** *Acta Neurol Scand* 1996;93:443–449
29. Ashwal S, Stringer W, Tomasi L, Schneider S, Thompson J, Perkin R. **Cerebral blood flow and carbon dioxide reactivity in children with bacterial meningitis.** *J Pediatr* 1990;117:523–530
30. Duncan R, Patterson J, Bone I, Kennedy PGE. **Single photon emission computed tomography in diagnosis of herpes simplex encephalitis.** *Lancet* 1988;2:515
31. Pexman JHW. **The angiographic and brain scan features of acute herpes simplex encephalitis.** *Br J Radiol* 1973;47:179–184
32. Tureen JH. **Cerebral blood flow and metabolism in experimental meningitis.** *Pediatr Infect Dis J* 1989;8:917–918
33. Täuber MG. **Brain edema, intracranial pressure and cerebral blood flow in bacterial meningitis.** *Pediatr Infect Dis J* 1989;8: 915–917
34. Heiss WD, Herholz K, Podreka I, Neubauer I, Pietrzyk U. **Comparison of 99m Tc-HMPAO SPECT with 18K-fluoromethane PET in cerebrovascular disease.** *J Cereb Blood Flow Metab* 1990;10: 687–697
35. Amlie-Lefond C, Kleinschmidt-DeMasters BK, Mahalingham R, Davis LE, Gilden DH. **The vasculopathy of varicella-zoster virus encephalitis.** *Ann Neurol* 1995;37:784–790
36. Feldmann M, Voth E, Dressler D, Henze T, Felgenhauer K. **99m Tc-Hexamethylpropylene amine oxime SPECT and X-ray CT in acute cerebral ischaemia.** *J Neurol* 1990;237:457–479
37. Raynaud C, Rancurel G, Tzourio N, et al. **SPECT analysis of recent cerebral infarction.** *Stroke* 1989;20:192–204
38. Quagliarello VJ, Wispelwey B, Long WJ, Scheld WM. **Recombinant human interleukin-1 induces meningitis and blood brain barrier injury in the rat: characterization and comparison with tumor necrosis factor.** *J Clin Invest* 1991;87:1360–1366
39. Koedel U, Bernatowitcz A, Paul R, Frei K, Fontana A, Pfister H-W. **Experimental pneumococcal meningitis: cerebrovascular alterations, brain edema, and meningeal inflammation are linked to the production of nitric oxide.** *Ann Neurol* 1995;37:313–323